

Determining activation energies and relaxation times of individual electron traps by scanning tunneling microscopy

Erica N. Schulman*

Department of Physics, Columbia University, New York, New York 10027

R. C. White

Department of Electrical Engineering, Columbia University, New York, New York 10027

(Received 9 February 1995; revised manuscript received 4 May 1995)

A method of determining the activation energies and relaxation times of electron traps is presented. The technique is applicable to traps across a broad bandwidth of switching frequencies, and can be easily automated. Examples are given, demonstrating precise determination of activation energy by scanning tunneling microscopy.

Electron traps play an important role in determining electrical properties, by introducing fluctuations in the number of carriers or modifying the local potential. Their effect is greatly enhanced for smaller systems, where microscopic features can dominate charge transport. The scanning tunneling microscope (STM) should be an extremely valuable tool for studying these effects,¹ due to the nanometer-scale resolution of the STM on many surfaces; such a small path for current flow renders the conductance extremely responsive to electron trapping and generation-recombination noise.² Despite its sensitivity, however, the STM has been used to explore electron trapping in only one system, thin layers of oxide on silicon.^{3,4} Until now the technique has been limited by the lack of a means of extracting precise physical values from STM data, particularly for traps outside of a narrow bandwidth of relaxation times.⁴ In this paper we present a simple experimental method with a quantitative theoretical framework that can determine activation energies and relaxation times of individual electron traps over a wide bandwidth with a high degree of precision.

The material used in these experiments, pyromellitic dianhydride-oxydianiline (PMDA-ODA), is a polyimide with particular importance to the microelectronics industry because of its low dielectric constant, thermal stability, planarizability, and compatibility with commercial packaging techniques.⁵ The observed conductivity⁶ in thin films of PMDA-ODA is not fully understood, but shallow-trap states localized on the carbon-oxygen bonds have been suggested,⁷ as well as contributions from resident impurities. Films were prepared on atomically flat graphite substrates with DuPont Pyralin PI-2540 diluted in N-methylpyrrolidinone (NMP), followed by a stepwise cure to 400 °C. Samples were analyzed by x-ray photoelectron spectroscopy (XPS).

Our STM uses a lever arm and stopper to control tip approach,⁸ with the piezoelectric controls in an orthogonal tripod arrangement. The current preamplifier is an Ithaco 1211 operated at a dynamic range of 100 nA. All experiments were performed at operational pressures of $<1 \times 10^{-10}$ Torr. To achieve the needed tunneling stability, tungsten tips were prepared with HF immersion⁹

and *in situ* field emission at 1000 V with 400–600 μA of current for 15 min. They were also checked on control samples of graphite and gold.

We were able to identify spatially localized, reproducible current fluctuations on the PMDA-ODA surface. For this purpose we mapped out fluctuation levels over the sample. At evenly spaced points during the topographic scan the tip was held still, and 50 current values were recorded at a sampling rate of 10 kHz. A ratio F of fluctuations to the setpoint current was defined as $F \equiv |(I_{\max} - I_{\min}) / I_{\text{setpoint}}|$. The ratio is very sensitive to extrema, but this crude approach works well for distinguishing between areas of stable and unstable tunneling. A topographic image (left) and simultaneously collected fluctuation map are shown in Fig. 1. Notably, the difference in fluctuation values between the white and black areas on the map is two orders of magnitude. The contrast between regions was constant over several hours.

A more quantitative analysis was performed by examining the variance and power spectral density of the tunneling current at a given point for different bias voltages (with the same magnitude of setpoint current). Strong instabilities, if present at that site, were only visible within

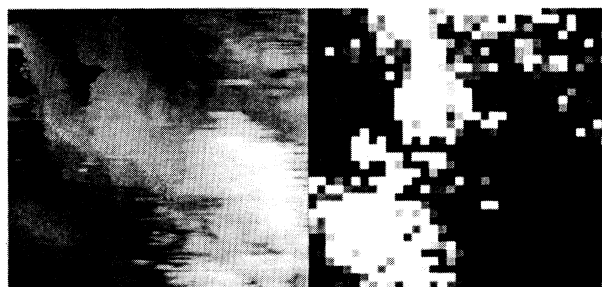


FIG. 1. Topographic image and corresponding fluctuation map recorded at a sample bias of 2V and a tunneling current of 1.1 nA. The lateral area is $50 \times 50 \text{ nm}^2$, with a greyscale range of 0.7 nm. Histogram equalization of the topographic image was performed to enhance vertical contrast. Each square on the fluctuation map represents one data point. The greyscale range goes from $F = 0\%$ (black) to $F \geq 2500\%$ (white).

a certain range of bias voltages. Outside that range, the variance was comparable to the system floor noise and the power spectrum was the expected $1/f$ form.^{10,11} Changes in the variance are shown in Fig. 2. A 100-mV change in bias voltage could affect the variance by an order of magnitude. Similarly dramatic effects can be seen in the power spectrum of Fig. 3, which switched from apparent white noise to the stable $1/f$ form.

For PMDA-ODA, conduction is often trap modulated.^{12,13} The system may be modeled as an extrinsic semiconductor with electron traps, with carrier fluctuations occurring between the conduction band and the traps. The variance of carriers in this case is given by¹⁴

$$\langle \Delta N^2 \rangle = \left[\frac{1}{N_0} + \frac{1}{N_{t1}} + \frac{1}{N_t - N_{t1}} \right]^{-1}, \quad (1)$$

where N is the number of carriers, N_0 is the number of carriers at thermal equilibrium, N_t is the number of traps, and N_{t1} is the number of occupied traps. The deviation from equilibrium, ΔN , is given by $\Delta N = N - N_0$. In general, these values are unknown. But if the number of carriers is much greater than the number of traps ($N_0 \gg N_t$), the first term drops out and

$$\langle \Delta N^2 \rangle = N_t \left[\frac{N_{t1}}{N_t} \right] \left[1 - \frac{N_{t1}}{N_t} \right], \quad (2)$$

so that the fractional trap occupancy N_{t1}/N_t becomes critical. The variance is highest for a situation in which half the traps are occupied. At either extreme the variance goes to zero. With spin degeneracy, the probability that a trap will be singly occupied can be obtained by statistical mechanics:

$$\frac{N_{t1}}{N_t} = \frac{2e^{-E_a^{\text{eff}}/kT}}{2e^{-E_a^{\text{eff}}/kT} + 1} = \frac{1}{\frac{1}{2}e^{E_a^{\text{eff}}/kT} + 1}, \quad (3)$$

where E_a^{eff} is the effective activation energy of the trap. E_a^{eff} will be affected by the electric field of the tip, and depends on the distance of the tip from the trap site.

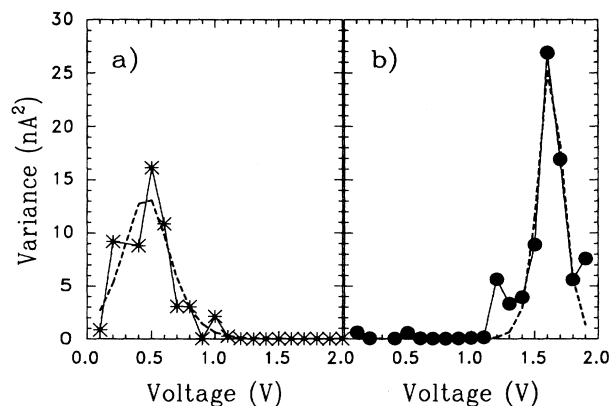


FIG. 2. Variance as a function of bias voltage for two regions on the polyimide surface. Each data point represents the variance of the mean 1.1-nA tunneling current recorded for 350 ms at 10 kHz.

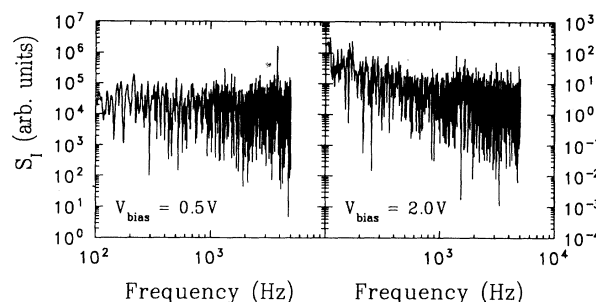


FIG. 3. Power spectrum densities for a point on the PMDA-ODA surface examined at a tunneling current of 1.1 nA and sample biases of 0.5 and 2.0 V. For this area, peak current fluctuations were observed at sample biases of 0.5 V, corresponding to Fig. 2(a).

We know $\langle \Delta I^2 \rangle = K \langle \Delta N^2 \rangle$, where I is the current due to the N carriers and K is a proportionality constant. Following previous authors,^{3,4} we assume that $E_a^{\text{eff}} = E_a^0 - \beta e V_{\text{bias}}$, where β (the electrical distance fraction) is the ratio of the change in energy of the trapping site to a change in eV_{bias} . (Because we operate at a positive sample bias, β represents the distance from the tip instead of the sample.) It is possible to numerically fit our variance data using the three previous equations with $kT = 0.025$ eV. There are three parameters: E_a^0 , β , and K . All parameters are unbounded during the numerical fit.

The exponent in Eq. (3) renders the curves very sensitive to the value of E_a^{eff} , and provides a rigorous test of the model. The first site examined corresponds to the upper middle region of Fig. 1. For the data shown in Fig. 2(a), $E_a^0 = 0.11 \pm 0.03$ eV within a 95% confidence interval.¹⁵ To our knowledge this is the most precise determination of trapping activation energy ever made by STM. β yields a value of 0.20 ± 0.06 . E_a^0 is physically reasonable and β is well below unity, consistent with a surface state. The scaling constant K is 54 ± 12 (nA)². The fit is shown as a dashed line, with good agreement with the experimental data.

A similar analysis was performed for the site of Fig. 2(b). The secondary peaks indicate that there may be additional traps nearby; this region (corresponding to the lower left of Fig. 1) appeared to have a dense trap concentration at high bias voltages. Our method is robust enough to give a good fit to the main peak, with $E_a^0 = 0.66 \pm 0.16$ eV, $\beta = 0.39 \pm 0.10$, and $K = 104 \pm 21$ (nA)².

For the area shown, there are two classes of current fluctuations: those in the upper middle region, which are most active at smaller bias voltages [Fig. 2(a)], and those in the lower left, which are most active at higher bias voltages [Fig. 2(b)]. The first class is confined to a location which shows some parallel orientation among the polymer chains. It is useful to compare this to the microscopic charge transport experiments that have been performed in anthracene pyromellitic dianhydride (A-PMDA).¹⁶ Similar to PMDA-ODA, this material is a donor-acceptor system with an aromatic, π -electron car-

rier as donor. Electron transport is dominated by movement of electrons between nearest-neighbor pyromellitimide units. There is a high degree of mobility between parallel chains, which act as adjacent shallow traps; this corresponds to our observations. The fluctuations of the second region occur in an area that is less topographically ordered, and they appear spatially isotropic. This is the manifestation of trapping sites in silicon oxide,^{3,4} and may represent impurities or defects.

We also wish to characterize the rate of the trapping events. The charge-carrier fluctuation due to generation and recombination can be described as $dN/dt = g(N) - r(N)$, where N is the number of carriers, g is the generation rate, r is the recombination rate, and t represents time. In general, both g and r are functions of N . The number of carriers at thermal equilibrium, N_0 , is defined by $dN/dt|_{N=N_0} = 0$ or $g(N_0) = r(N_0)$. We may define deviations in g and r , using a Taylor's-series expansion and an assumption of intrinsic fluctuation in the rates, e.g.,

$$g(N) = g(N_0) + \frac{dg}{dN} \Delta N + \Delta g(t). \quad (4)$$

We may now rewrite the rate equation in terms of ΔN :

$$\begin{aligned} \frac{d\Delta N}{dt} &= - \left[\frac{dr}{dN} - \frac{dg}{dN} \right] \Big|_{N=N_0} \Delta N + \Delta g(t) - \Delta r(t) \\ &= - \frac{\Delta N}{\tau} + \Delta g(t) - \Delta r(t), \end{aligned} \quad (5)$$

where

$$\frac{1}{\tau} = \left[\frac{dr}{dN} - \frac{dg}{dN} \right] \Big|_{N=N_0}. \quad (6)$$

τ defines the relaxation time for the system. The value of τ can be experimentally determined by the power spectrum.

To obtain the relationship between the power spectrum density and τ , we use the Langevin method¹⁷ and perform the expansion for Eq. (5):

$$\begin{aligned} \Delta N(t) &= \sum_{n=-\infty}^{\infty} a_n \exp(j\omega_n t), \\ \Delta g(t) &= \sum_{n=-\infty}^{\infty} b_n \exp(j\omega_n t), \\ \Delta r(t) &= \sum_{n=-\infty}^{\infty} c_n \exp(j\omega_n t). \end{aligned} \quad (7)$$

Looking at terms with common factors of $\exp(j\omega_n t)$,

$$a_n = \frac{\tau}{1 + j\omega_n \tau} (b_n - c_n), \quad (8)$$

which yields a power spectrum

$$S_N(f) = \frac{\tau^2}{1 + \omega^2 \tau^2} [S_g(f) + S_r(f)]. \quad (9)$$

$\Delta g(t)$ and $\Delta r(t)$ were assumed to be a result of shot

noise, so $S_g(f) = 2g(N_0)$.¹⁷ Since $g(N_0) = r(N_0)$, the spectrum may be rewritten as

$$S_N(f) = \frac{4g(N_0)\tau^2}{1 + \omega^2 \tau^2}, \quad (10)$$

or in terms of the current as

$$S_I(f) = \frac{I_0^2}{N_0^2} S_N(f) = 4 \frac{I_0^2 g(N_0)}{N_0^2} \frac{\tau^2}{1 + \omega^2 \tau^2}. \quad (11)$$

The variance in N may be expressed as¹⁷

$$\langle \Delta N^2 \rangle = \frac{g(N_0)}{dr(N_0)/dN - dg(N_0)/dN} = g(N_0)\tau, \quad (12)$$

and therefore

$$S_I(f) = 4 \frac{I_0^2}{N_0^2} \langle \Delta N^2 \rangle \frac{\tau}{1 + \omega^2 \tau^2}. \quad (13)$$

In Fig. 3(a) the spectrum appears flat for low frequencies, as predicted for $\omega\tau \ll 1$. For $\omega\tau \gg 1$, however, the spectrum should have a slope of -2 . We can predict the rolloff frequency given the magnitude of $S_I(f)$ in the dc limit. At zero frequency,

$$\tau = \frac{S_I(0)N_0^2}{4I_0^2 \langle \Delta N^2 \rangle}. \quad (14)$$

The ratio N_0/I_0 is given by $1/\sqrt{K}$. At the optimal bias voltage, we assume the maximum variance, which is $\frac{1}{4}$ for a single trap. $S_I(0)$ is given by the identity $S_I(0) = \langle \Delta I^2 \rangle \Delta t$, where Δt is the time between current samples (in this case 0.1 ms). This relationship was confirmed by the experimental data. For the fluctuator of Fig. 2(a), $S_I(0) \sim 3 \times 10^{-3}$ s(nA)², which implies $\tau \approx 6 \times 10^{-5}$ s. Therefore the flat spectral power density is expected over our accessible frequencies of < 5 kHz. $\tau \approx 2 \times 10^{-6}$ s for the fluctuator of Fig. 2(b), which had a similar spectral power density.

We have been able to determine individual electron trap activation energies and relaxation times using STM and a quantitative method of analysis. Since the low-frequency limit of current noise is the critical piece of experimental data, this technique is suitable for characterizing traps with relaxation times within or above the measurement bandwidth. In addition, it is no longer necessary to fit the time-series spectrum of the tunneling current at each bias voltage, allowing for more accurate and efficient experiments.

ACKNOWLEDGMENTS

We would like to thank Kevin Delin for useful discussions and suggestions. The support of IBM, DuPont, the National Science Foundation (Grants Nos. CHE-9158375 and CHE-9410527), and the Office of Naval Research (Grant No. N-00014-94-J-1630) is gratefully acknowledged.

- *Present address: Department of Chemistry, 152 Davey Laboratory, Pennsylvania State University, University Park, PA 16802. Electronic address: ens1@psuvm.psu.edu
- ¹M. B. Weissman, *Rev. Mod. Phys.* **60**, 537 (1988).
- ²F. W. Schmidlin, *J. Appl. Phys.* **37**, 2823 (1966).
- ³M. E. Welland and R. H. Koch, *Appl. Phys. Lett.* **48**, 724 (1986).
- ⁴R. H. Koch and R. J. Hamers, *Surf. Sci.* **181**, 333 (1987).
- ⁵J. J. Licari, *Plastic Coatings for Electronics* (McGraw-Hill, New York, 1970).
- ⁶R. Haight, R. C. White, B. D. Silverman, and P. S. Ho, *J. Vac. Sci. Technol. A* **6**, 2188 (1988).
- ⁷J. P. LaFemina, *Chem. Phys. Lett.* **159**, 307 (1989).
- ⁸J. E. Demuth, R. J. Hamers, R. M. Tromp, and M. E. Welland, *J. Vac. Sci. Technol. A* **4**, 1320 (1986).
- ⁹L. A. Hockett and S. E. Creager, *Rev. Sci. Instrum.* **64**, 263 (1993).
- ¹⁰T. Tiedje, J. Varon, H. Deckman, and J. Stokes, *J. Vac. Sci. Technol. A* **6**, 372 (1988).
- ¹¹R. Möller, A. Esslinger, and B. Koslowski, *Appl. Phys. Lett.* **55**, 2360 (1989).
- ¹²G. M. Sessler, B. Hahn, and D. Y. Yoon, *J. Appl. Phys.* **60**, 318 (1986).
- ¹³P. K. C. Pillai and B. L. Sharma, *Polym. Rep.* **32**, 3861 (1979).
- ¹⁴R. E. Burgess, *Proc. Phys. Soc. B* **69**, 1020 (1956).
- ¹⁵The fit was performed using PSI-Plot, Poly Software International, P. O. Box 526368, Salt Lake City, UT 84152. The Marquardt-Levenburg method was used.
- ¹⁶D. Massa and N. Karl, *Mol. Cryst. Liq. Cryst.* **95**, 93 (1989).
- ¹⁷A. van der Ziel, *Noise in Measurements* (Wiley, New York, 1976).

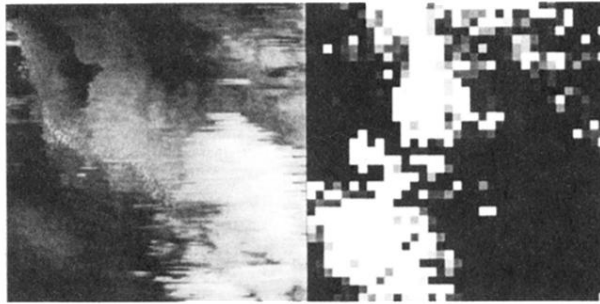


FIG. 1. Topographic image and corresponding fluctuation map recorded at a sample bias of 2V and a tunneling current of 1.1 nA. The lateral area is $50 \times 50 \text{ nm}^2$, with a greyscale range of 0.7 nm. Histogram equalization of the topographic image was performed to enhance vertical contrast. Each square on the fluctuation map represents one data point. The greyscale range goes from $F = 0\%$ (black) to $F \geq 2500\%$ (white).